國　立　清　華　大　學

碩士論文

我的論文標題 (中文)

My thesis title (Chinese)

系　　所：物理研究所

學　　號：105022511

研 究 生：韓正忻　　　(Cheng-Hsin Han)

指導教授：徐百嫻　博士　(Prof. Pai-Hsien Jennifer Hsu)

中 華 民 國 一〇七 年 十二 月

Todo list

“Todo List” will hide when set \setboolean{publish}{*true*} in config.tex.

我的論文標題 (中文)

摘要

在此寫上你的中文摘要。

關鍵字：關鍵字, 論文, 樣板, 讓我畢業

摘要

My thesis title (Chinese)

Abstract

Write your English abstract here.

Keywords: Keyword, Thesis, Template, Graduate me

Acknowledgement

Thanks NCU, and sppmg's LaTeX template_**sppmg/tw_thesis_template_????**.

Contents

List of Figures

page

List of Tables

Glossary

Use table for symbol list. You can also use package “nomencl” (simple) or “glossaries” (powerful). see packages document or my tutorial (but it’s Chinese).

Glossary

VIM	:	The best guy’s editor
Emacs	:	The God’s editor
CTAN	:	Comprehensive TeX Archive Network, ctan.org

Chapter 1

Introduction

(You can copy “chapter_template.tex” or “chapter_template_demo.tex” to create new sub-file(chapter).)

Write your Introduction here. eg,

I don’t want my chaste thesis impinge by M$. But LaTeX is little hard.

Chapter 2

The ATLAS detector

2.1 Coordinates

The ATLAS (**A** **T**oroidal **L**HC **A**pparatu**S**) experiment is one of the seven detector in Large Hadron Collider (LHC) at CERN (European Organization for Nuclear Research). Its cylindrical symmetry and end caps covers nearly 4π in solid angle.

A coordinate system is used to describe every recorded signals nearby. The origin is set at the center of the detector, or the interaction point (IP). The x-axis points toward the center of the LHC ring; the y-axis points vertically upward; the z-axis points along one of the beam pipe direction such that a right-handed coordinate sysetem is created.

A modified version of cylindrical coordinate is more commonly used in the experiment. The pseudorapidity $\eta \equiv -\ln\tan(\theta/2)$, in which θ is the polar angle in cylindrical coordinate, is used to decribe the angle between the z-axis and the direction of interest. (r, ϕ) is the same system to describe the tranverse plane, with ϕ being the azimuthal angle. In addition, the cone size variable, which is used in object selection and reconstruction, is defined as $\Delta R \equiv \sqrt{(\Delta\phi)^2 + (\Delta\eta)^2}$.

2.2 Components of ATLAS

Depending on its function, the components are categorized into four parts - inner detector, calorimeters, muon spectrometer, and the magnetic system. Apart from these, there are three levels of triggers which are designed to reduce the amount of data and also keep the signals of interest. Figure 2.1 shows the schematic positions and 2.2 shows the side view of each components of ATLAS. The solenoidal magnets surround the inner detector while the toroidal magnets affects the signals in the muon spectrometer. Thses two magnets form the magnetic system. The others consist of smaller layers or components which is described in the following.

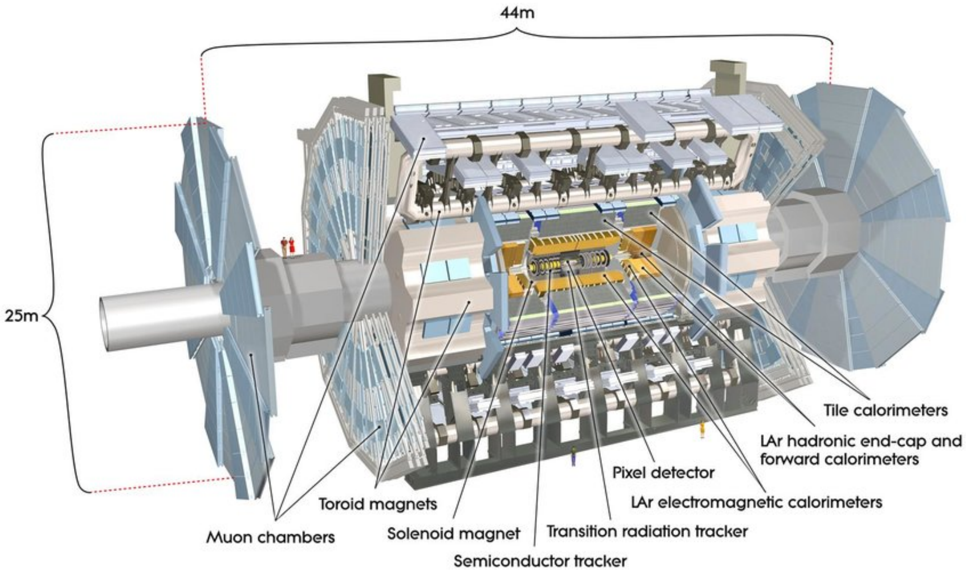

Figure 2.1: Schematic plot of the ATLAS detector as well as the positions of its components.

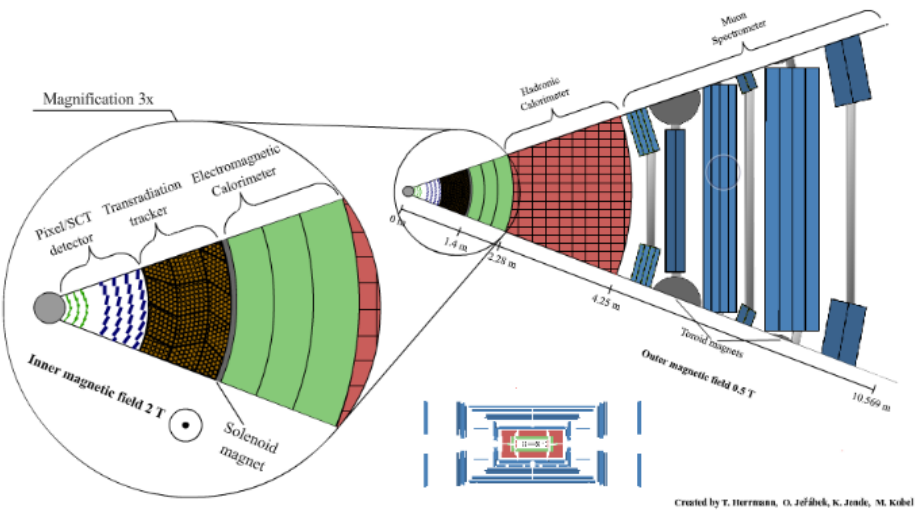

Figure 2.2: Schematic plot of the side view of the ATLAS detector.

2.2.1 Inner Detector

Beginning few centimeters from the IP, the inner decector's main function is to track the trace of charged particles by their interations with the materials. A 2T magnetic field, which is generated from the solenoidal magnets surrounding the whole inner detector, causes the charged ones to bend. Based on the directions and the curvatures, one can determine their charges and momenta preliminarily. The inner detector comprises three parts - the pixel detector, the semi-conductor tracker (SCT), and the transition rediation tracker (TRT).

Located at the innermost part, the pixel detector contains four layers of modules, which is made up silicon, in the direction perpendicular to the beam. It covers pseudorapidity range $|\eta| < 2.5$ and its proximity to the IP is meant to measure extremely precise trace of the charged particles. Made up of similar material, three disks are at each end cap of the detector.

The semi-conductor tracker, having a similar concept and function to the pixel detector, lies in the middle part of the inner detector. Although having a resemblance to the pixel detector, the SCT is in a long and narrow strip-shape rather than small pixels and covers the perpendicular directions to the beam instead of nearly full coverage. The SCT, which overlays a larger area than the pixel detector does, has more sampled points and thus is of great importance on tracking the transverse directions with roughly the same accuracy compared to the pixel detector.

The outermost component, TRT, includes straw tube trackers and transition radiation detectors. Though its precision in tracking is not as high and its coverage in pseudorapidity, about $|\eta|< 2.0$, is not as wide as those of the other two components, TRT possesses transition radiation detection capability, which is useful for identifying charged particles. Since the lighter particles tend to have higher speed, which generates greater transition radiation, electrons and positrons, the lightest charged particles, would leave strong signals in TRT.

2.2.2 Calorimeters

Outside the solenoidal magnet, which envelops the inner detector, are the calorimeters. By absorbing the particles, the calorimeters measure the energies of them. Two layers of components compose the calorimeter systems, the inner electromagnetic (EM) calorimeter and the outer hadronic calorimeter.

As its name suggests, the EM calorimeter absorbs energies from particles that interact electromagnetically, including photons and charged particles. A pseudorapidity of range $|\eta| < 3.2$, which includes the barrel and end cap, is covered by high-granularity lead/liquid argon(LAr) EM calorimeter. In addition, a LAr persampler which is meant to correct the energy loss in materials of the calorimeters covers $|\eta| < 1.8$. For the forward region, which has the range $3.1 < |\eta| < 4.9$, a LAr EM calorimeter with copper is also deployed.

Hadronic calorimeter, although it is less precise in both energy magnitude and localization than EM calorimeter, absorbs energies from the particles that interact via strong force. Hadrons, which is identified as jets, and τ leptons, which mainly decay hadronically, are the targeted particles of hadronic calorimeter. Steel/scintillator-tile covering $|\eta| < 1.7$, two copper/LAr end cap calorimeters overlaying $1.5 < |\eta| < 3.2$, and a forward-regional $(3.1 < |\eta| < 4.9)$ tungsten absorbers constitute the hadronic calorimeter.

2.2.3 Muon Spectrometer

Muon spectrometer, which is meant to provide more precise measurement of muon momenta and tracks, surrounds the calorimeters. Due to the fact that few particles rather than muons passes through it, muon spectrometer also has a function of identifying the muons. A magnetic field, provided by three toroidal magnets and thus is not uniform, creates a curve in muon tracks, which can be made use of measuring the momenta. Detectors with triggers provide the identification and momenta measurements of the muons within the range $|\eta| < 2.4$; over a thousand precision tracking chambers covering $|\eta| < 2.7$ serve the muon spatial measurements.

2.2.4 Trigger System

A trigger is a set of device which sets thresholds on some physical quantities such as momenta and positions. If the threshold of one event is met, one keeps it; otherwise one abandons it. The ATLAS triggers consist of three levels. The first level is hardware based while the other two are software based. From roughly 1 billion events per second, these three triggers combined select about few hundreds interesting. Namely, the interaction rate is reduced from 1 GHz to few hundreds Hz.

Chapter 3

Object Selection and Reconstruction

Signals recorded in the ATLAS detector are categorized or reconstructed as pysical objects, which could be further used in the analyses. The reconstruction and definition of objects used in this study are listed in the following.

3.1 Jets

3.2 Leptons

Leptons are used to categorized the regions selected in this analysis, which would be covered in the next chapter. Requirements of each flavor are explained in the following and summarized in table.3.1.

Table 3.1: The summarization of lepton selection and reconstruction. The rightmost column are the requirements for the reconstructed small-R jet that decays from a τ-lepton candidate.

flavor	e		μ		τ
categorization	baseline	signal	baseline	signal	-
p_T (GeV)	> 7	> 27	> 7	> 25	> 20
$\|\eta\|$	(0, 2.47)		(0, 2.7)	(0, 2.5)	$(0,\ 1.37) \cup (1.52,\ 2.5)$
ID	Loose		Loose (0/2-muon) Medium (1-muon)		Loose
transverse impact parameter	$d_0/\sigma(d_0) < 5$		$d_0/\sigma(d_0) < 3$		$\|d_0\| < 1$ mm
$\|z_0 \sin(\theta)\|$ (mm)	< 0.5				< 1.5
Additional	-				one to four track-jets $\Delta\phi(\tau, \not{E}_T) < \frac{\pi}{8}$

3.2.1 Electrons

Electron candidates are reconstructed from the energy deposits in EM calorimeter that match a track recorded in the inner detector. In addition, there is a likelihood-based (LH) algorithm, which further makes use of multivariable analysis (MVA), applied for the electron ID. Three levels of ID operating point, loose, medium and tight, are povided; among them, loose ID is used in this study for the electrons. Moreover, electrons are divided into two groups, the baseline electrons, whose transverse momentum, or p_T, exceed 7 GeV, and the signal electrons, which requires a tighter threshold of $p_T > 27$ GeV. All candidates within $|\eta| < 2.47$ are considered. Finally, requirements of the impact parameter are considered, both in the transverse and logitudinal directions. For the former, the relative resolution, which is the fraction of the transverse impact parameter d_0 and its resolution $\sigma(d_0)$, has an upper bound of 5. For the latter, the value $|z_0 \sin(\theta)| < 0.5$ mm is set, where z_0 is the point closet to the vertex along the logitudinal axis and θ is the polar angle of the track.

3.2.2 Muons

Muon candidates, also divided into baseline and signal muons, are reconstructed with high dependence of inner detector and the muon spectrometer. Signal muons, whose p_T exceed 27 Gev, are more likely to leave tracks in the inner detector, and thus shall be found in $|\eta| < 2.5$. For baseline muons, which have a looser p_T threshold of 7 GeV, leaving signals in the inner detector is not required and thus are within $|\eta| < 2.7$, which is the range of the muon spectrometer. On top of that, the impact parameter must be consistent with the reconstructed location of the collision, or the primary vertex. $d_0/\sigma(d_0) < 3$ and $|z_0 \sin(\theta)| < 0.5$ mm are set. Finally, a loose ID is used for the zero-lepton and two-muon channel whilst the one-muon channel makes use of a medium ID for the muons in this analysis. These channels would be covered in the upcoming chapter.

3.2.3 Taus

τ-leptons, whose decay length is few μm, barely reach the ATLAS detector and thus are mainly reconstructed from their decay products. Due to the fact that most of the τ-leptons decay into hadrons, the τ-lepton candidates are reconstructed from jets. The transverse impact parameter, $|d_0| < 1$ mm, and the logitudinal one, $|z_0 \sin(\theta)| < 1.5$ mm, are set for the jet tracks and the τ vertex. The threshold on the p_T of the jets is set at 20 GeV; the range of $|\eta| < 2.5$, excluding $1.37 < |\eta| < 1.52$, which is the region between the barrel and the forward region, or the crack region, is also required. Furthermore, the ID is built on a boosted decision tree (BDT) that makes use of the information from the tracks and the calorimeter. The loose working point on the τ-leptons is used. Finally, the small-R jet is required to contain one to four track-jets and within a range of $\Delta\phi < \frac{\pi}{8}$ with the missing transverse energy (MET, E_T^{miss} or $\not{E}_T$) in order to suppress the W-boson-decayed τ-leptons.

3.3 Missing Transverse Energy

3.4 Overlap Removal

Chapter 4

Conclusion

I am free, I am not own by M$.

Chapter 5

Chapter name(demo)

Content of chapter

Content Content Content.

5.1 Section name

Content of section

Content Content Content

5.1.1 Subsection name

Content of subsection

Content Content Content

5.1.1.1 Subsubsection name

Content of subsubsection

Content Content Content

5.1.1.1.1 Paragraph name Content of paragraph

Content Content Content

Subparagraph name Content of subparagraph

Content Content Content

Chapter 6

Test demo

First line. (next line in LaTeX)still first line.
Second line.

Chapter 7

figure

7.1 Insert single figure(by sppmg's tool)

Figure 7.1: caption

7.2 Insert figures

(a) caption_1

(b) caption_2

(c) caption_3

Figure 7.2: caption, use “(b)” get ID of subfigure(this ID is Debian) in caption

Chapter 8

Table

8.1 Simple table

Table 8.1: Solution

Component	Concentration(mM)
$CaCl_2$	118.0

8.2 Auto break line table

short	short short
long	long long long long long long long long long long

Appendix A

List of device

Table A.1: List of device

device	Model	Description
Linux	Debian 9	Best of best of best OS
Windows	10	Best of Best tool to prevent the aging of brain.

Appendix B

Solutions

B.1 The solution

Table B.1: The solution

Component	Concentration(mM)
NaCl	1.0
$CaCl_2$	2.0
NaCl	1.0
$CaCl_2$	2.0

Appendix C

Code

C.1 C

Code C.1: hello_world_c.c

```c
#include <stdio.h>
main()
{
    printf("hello, world\n");
}
```

C.2 Matlab

Code C.2: hello_world_matlab.m

```matlab
fprintf('hello, world\n');
```

C.3 IDL

Code C.3: hello_world_idl.pro

```idl
print,"hello, world"

end
```